Physics

Physics fields

Okayama University *Year* 2005

Fabrication of field-effect transistor device with higher fullerene, C_{88}

Takayuki Nagano* Hiroyuki Sugiyama† Eiji Kuwahara‡
Rie Watanabe** Haruka Kusai††
Yoko Kashino‡‡ Yoshihiro Kubozono Prof.§

*Okayama University
†Okayama University
‡Okayama University
**Okayama University
††Okayama University
‡‡Okayama University
§Okayama University, kubozono@cc.okayama-u.ac.jp

Fabrication of field-effect transistor device with higher fullerene, C_{88}

Takayuki Nagano, Hiroyuki Sugiyama, Eiji Kuwahara, Rie Watanabe,
Haruka Kusai, Yoko Kashino and Yoshihiro Kubozono[a)]
Department of Chemistry, Okayama University, Okayama 700-8530, Japan and CREST, Japan Science and Technology Agency , Kawaguchi, 322-0012, Japan

A fullerene field-effect transistor (FET) device has been fabricated with thin films of C_{88}, and n-channel normally-on depletion-type FET properties have been found in this FET device. The C_{88} FET exhibited a high mobility, μ, of 2.5 x 10^{-3} cm^2 V^{-1} s^{-1} at 300 K, in fullerene FETs. The carrier transport showed a thermally-activated hopping transport. The n-channel normally-on FET properties and the hopping transport reflect the small mobility gap and low carrier concentration in the channel region of C_{88} thin-films.

[a)] Electronic mail: kubozono@cc.okayama-u.ac.jp

A number of field-effect transistors (FETs) have been fabricated with thin films of organic molecules, and their properties have been studied for the next-generation electronics during the past 10 years.[1,2] The mobilities, μ, of the FETs with organic molecules (organic FETs) are generally lower than those, ~ 1000 $cm^2 V^{-1} s^{-1}$, of the conventional FETs with inorganic materials (inorganic FETs). However, the organic FETs are well known to have many advantages such as large-area coverage, structural flexibility, and low-temperature and low-cost processing, in comparison with inorganic FETs.

The highest μ value in p-channel organic thin-film FET devices was 1.5 $cm^2 V^{-1} s^{-1}$ for the pentacene thin-film FET.[3] Recently, the μ value reached to 8 - 20 $cm^2 V^{-1} s^{-1}$ in the rubrene single-crystal FET device exhibiting p-channel behavior.[4-6] On the other hand, the highest μ value in n-channel organic FET devices was 0.6 cm^2 V^{-1} s^{-1} for the *N,N'*-dialkyl-3,4,9,10-perylene tetracalboxylic diimide derivative FET device.[7] These μ values are comparable to those of the recent amorphous Si FETs.[1,2]

The fullerene FET was first fabricated with thin films of C_{60} by Haddon *et al*.[8] This FET device showed the high μ value of 0.08 – 0.3 $cm^2 V^{-1} s^{-1}$. Subsequently, the C_{70} FET device was fabricated and the n-channel properties were observed with the μ of 2 x 10^{-3} cm^2 V^{-1} s^{-1}.[9] Recently, the μ value for the C_{60} thin-film FET reached to 0.56 $cm^2 V^{-1} s^{-1}$ when the FET properties were measured under 10^{-9} Torr without an exposure to air.[10] Thus, the high μ value implies that the C_{60} FET can play an important role in future applications towards the practical organic FET devices.

We have examined to fabricate the FET devices with thin films of various types of higher fullerenes and endohedral metallofullerenes in order to improve their FET properties.[11-14] All

FET devices with higher fullerenes and endohedral metallofullerenes showed n-channel normally-on properties which originated from high bulk currents caused by small gap energies, E_g's. Thus, the observed properties reflect the intrinsic nature of fullerenes used as active layer. Therefore, the fabrications and characterizations of the FET devices with a series of higher fullerenes and endohedral metallofullerenes are indispensable to know their electronic properties and possibility of application as electronic materials. In the present study, we have first fabricated a high-performance FET device with higher fullerene, C_{88}. The electronic properties of giant fullerenes such as C_{88} have never been studied because of a difficulty in obtaining pure solid-samples. Therefore, the present study is the first approach to the electronic properties of giant fullerenes.

The schematic representation of C_2-isomer (#7), $C_2(7)$, of C_{88} and the cross-sectional view of the C_{88} FET device are shown in Fig. 1(a); the $C_2(7)$-C_{88} is one of seven C_2 isomers of C_{88}.[15] The C_{88} sample was purified by high performance liquid chromatography with toluene as eluent, after a Soxhlet-extraction of the soot containing C_{88} with 1,2,4-*tri*-chlorobenzene, where the soot was prepared by an arc-discharge of carbon graphite rods containing Eu_2O_3. The time-of-flight mass spectrum of the purified sample is shown in Fig. 1(b), which exhibited only a single peak for C_{88}. The purified sample may contain some isomers since the isomer-separation of C_{88} sample was not performed. The commercially available SiO_2/Si(100) wafer was used as a substrate after washing with acetone, methanol and H_2SO_4/H_2O_2. The SiO_2/Si substrate was treated with hexamethyldisilazane (HMDS) to form a hydrophobic surface. The thickness and capacitance, C_0, of SiO_2 were 420 nm and 8.2 x 10^{-9} F cm^{-2}, respectively. The thin film of C_{88} was formed by a thermal deposition under a vacuum of 10^{-8} Torr. The channel length, L, and the channel width, W, of this device were 30

and 3000 μm, respectively. The FET properties of the C_{88} FET device were measured under 10^{-6} Torr after annealing for 13 h at 120˚C under 10^{-6} Torr.

The drain current, I_D, *vs.* drain-source voltage, V_{DS}, plots for the C_{88} FET at 300 K are shown in Fig. 1(c). The plots show n-channel normally-on depletion-type FET properties. The I_D –V_G plot at V_{DS} = 20 V is also shown in Fig. 1(d). The I_D increases with an increase in V_G from –30 to 100 V. It should be noted that the channel conductance decreases by applying the negative V_G, due to the depletion of carriers in the channel. The μ value at 300 K for the C_{88} FET was estimated to be 2.5 x 10^{-3} cm^2 V^{-1} s^{-1} from the I_D - V_G plot above V_G = 60 V (Fig. 1(d)) with the equation (1) for $V_{DS} << V_G - V_T$,

$$I_D \sim (\mu W C_0 / L)(V_G - V_T)V_{DS,} \quad (1)$$

where V_T refers to the threshold voltage.[16] This μ value is the highest one next to that of the C_{60} FET among fullerene FETs. The V_T was estimated to be –142 V from the I_D-V_G plot (Fig. 1(d)). Furthermore, the μ and V_T values were estimated from the I_D – V_G plots at V_{DS} of 5, 10 and 30 V in order to confirm the validity of the very high negative value of V_T. The μ and V_T values were almost consistent with each other, and the same as those at V_{DS} = 20 V, showing that the μ and V_T values are reliable. The negative V_T of -142 V supports that the C_{88} FET is normally-on type. Such a depletion-type property was observed for C_{82} and C_{84} FETs.[12,13] The on-off ratio was estimated to be ~7 from the I_D at V_G = 100 V and that at V_G = -30 V. This value is also the best one at room temperature among normally-on type FET devices: ~2.1 for C_{82}, ~6 for C_{84} and ~3.1 for Pr@C_{82}.[12-14] These FET parameters show that C_{88} is the second

best material for active layer of FET among fullerenes.

Here, we have investigated the variation of μ for the applied V_G with the equation (2),

$$\mu \sim (L / (WC_0V_{DS}))\, dI_D/dV_G, \quad (2)$$

in order to confirm whether the FET parameters obtained reflect the intrinsic carrier transport in the C_{88} FET; if the μ value is not influenced by the V_G, the FET parameters, inclusive of the μ, can closely be associated with the intrinsic nature of the carrier transport in the C_{88} FET device.[17] The V_G dependence of μ value estimated with eq. (2) is shown in Fig. 2, and the μ value above V_G of 60 V is almost the same as the μ, 2.5 x 10^{-3} cm^2 V^{-1} s^{-1}, estimated with eq. (1). The μ value ranges from 2 x 10^{-3} to 6.5 x 10^{-3} cm^2 V^{-1} s^{-1} at V_G of –30 ~ 100 V, as shown in Fig. 2. This result implies that the FET properties are partly influenced by the V_G-dependence of resistance of source and drain contacts owing to two-probe measurements used in this study.

The I_D –V_{DS} plots at 230 K for the C_{88} FET is shown in Fig. 3(a), and the I_D – V_G plot is shown in Fig. 3(b). The μ and V_T were estimated to be 7.2 x 10^{-4} cm^2 V^{-1} s^{-1} and –50 V, respectively, with eq. (1). The on-off ratio was 24, whose value was larger by three times than that at 300 K. The I_D at V_G = 0 V was lower by one order of magnitude than that at 300 K. Thus a decrease in bulk current can lead to an increase in the on-off ratio at 230 K. The μ increased exponentially with an increase in temperature, T, up to 350 K (Fig. 3(c)), and the μ value reached to 8.0 x 10^{-3} cm^2 V^{-1} s^{-1} at 350 K. The plot of μ - T shows that the channel conduction of the C_{88} FET device follows a thermally-activated hopping-transport model (μ

~ exp-E_a/k_BT). The activation energy E_a was estimated to be 0.13 eV from the lnμ - 1/T plot shown in the inset of Fig. 3(c). This value is consistent with those, 0.14 and 0.13 eV, for the C_{82} and C_{84} FETs, respectively,[12,13] while the value is smaller than that, 0.22 eV, for the Pr@C_{82} FET.[14] These results show that the FET properties of the higher fullerene FETs are similar with each other. Further, we can point out that the properties of higher fullerenes are different from those of endohedral metallofullerenes; for example, the μ values, ~ 10^{-3} cm^2 V^{-1} s^{-1}, of higher fullerene FETs are higher by one order of magnitude than those, ~10^{-4} cm^2 V^{-1} s^{-1}, of endohedral metallofullerenes, and the depletion properties can be more clearly observed in the higher fullerenes than endohedral metallofullerenes.[11-14] The high μ for the higher fullerenes originates from the fact that intermolecular overlap of the lowest unoccupied molecular orbitals (LUMOs) of the higher fullerenes is large because of the delocalized π character. Since more critical factor is the crystallinity of the thin films, it is necessary to investigate the crystallinity of thin films of higher fullerenes and endohedral metallofullerenes in detail.

The bulk current increases exponentially with increasing T, where the I_D at V_G = 0 V and V_{DS} = 20 V was used as bulk current. The gap energy, E_g, was estimated to be 0.42 eV from the lnI_D – 1/T plot, and the E_g is consistent with those, 0.43 and 0.55 eV, for C_{82} and C_{84}, respectively, estimated from resistivity ρ – T plot.[12,13] The E_g cannot be attributed to the band gap but mobility gap, as suggested by Shiraishi et al.[18] The V_T decreases monotonically with increasing T up to 350 K (Fig. 3(d)). Such T dependence can be reasonably explained by an increase in bulk current described above. The V_T increased to ~0 V at 160 K. Thus, the FET property changes from normally-on to normally-off-like with decreasing T owing to a

decrease in bulk current.

In the present study, some intrinsic characters for the C_{88} FET have been clarified, although the V_G dependence of resistance of source and drain contracts partly affects the FET properties observed. The normally-on FET properties found in this device reflects the small E_g for the C_{88} thin-films. The delocalized LUMOs in C_{88} produce the larger μ than those in the endohedral metallofullerene FETs. Furthermore, the hopping conduction observed in the C_{88} thin-films originates from low carrier concentration of at most 5×10^{12} cm^{-2} at V_G = 100 V, *i.e.*, the metallic conduction never occurs at such low concentration because 0.05 electrons are exclusively injected into a C_{88} molecule. Therefore, the high carrier injection is very important for a realization of metallic transition, and one of the approaches to high carrier injection is to use high dielectric materials for the FET devices. In the present study, the electronic properties of C_{88} have been investigated, and its possibility of applications for electronic materials has been indicated from the highest FET performance next to the C_{60} FET.

This work was in part supported by a Grant-in-Aid (15350089) from MEXT, Japan and by Mitsubishi Foundation.

1. C. D. Dimitrakopoulos and D. J. Mascaro, IBM J. Res. Dev. **45**, 11 (2001).
2. C. D. Dimitrakopoulos and P. R. L. Malenfant, Adv. Mater. **14**, 99 (2002).

3. Y.-Y. Lin, D. J. Gundlach, S. F. Nelson, and T. N. Jackson, IEEE Electron Device Lett. **18**, 606 (1997).

4. J. Takeya, T. Nishikawa, T. Takenobu, S. Kobayashi, Y. Iwasa, T. Mitani, C. Goldmann, C. Krellner, and B. Batlogg, Appl. Phys. Lett. **85**, 5078 (2004).

5. V. C. Sundar, J. Zaumseil, V. Podzorov, E. Menard, R. L. Willett, T. Someya, M. E. Gershenson, and J. A. Rogers, Science, 303, 1644 (2004).

6. V. Podzorov, E. Menard, A. Borissov, V. Kiryukhin, J. A. Rogers, and M. E. Gershenson, Phys. Rev. Lett. 93, 086602 (2004).

7. P. R. L. Malenfant, C. D. Dimitrakopoulos, J. D. Gelorme, L. L. Kosbar, T. O. Graham, A. Curioni, and W. Andreoni, Appl. Phys. Lett. **80**, 2517 (2002).

8. R. C. Haddon, A. S. Perel, R. C. Morris, T. T. M. Palstra, A. F. Hebard, and R. M. Fleming, Appl. Phys. Lett. **67**, 121 (1995).

9. R. C. Haddon, J. Am. Chem. Soc. **118**, 3041 (1996).

10. S. Kobayashi, T. Takenobu, S. Mori, A. Fujiwara, and Y. Iwasa, Appl. Phys. Lett. **82**, 4581 (2003).

11. T. Kanbara, K. Shibata, S. Fujiki, Y. Kubozono, S. Kashino, T. Urisu, M. Sakai, A. Fujiwara, R. Kumashiro, and K. Tanigaki, Chem. Phys. Lett. **379**, 223 (2003).

12. Y. Kubozono, Y. Rikiishi, K. Shibata, T. Hosokawa, S. Fujiki, and H. Kitagawa, Phys. Rev. B. **69**, 165412 (2004).

13. K. Shibata, Y. Kubozono, T. Kanbara, T. Hosokawa, A. Fujiwara, Y. Ito, and H. Shinohara, Appl. Phys. Lett. **84**, 2572 (2004).

14. T. Nagano, E. Kuwahara, T. Takayanagi, Y. Kubozono, and A. Fujiwara,Chem. Phys. Lett. to be published.

15. P. W. Fowler and D. E. Manolopoulos, *An Atlas of Fullerenes* (Oxford Press, Oxford, 1995).

16. S. M. Sze, Semiconductor Devices, Physics and Technology (Wiley, New York, 2002).

17. R. W. I. de Boer, M. E. Gershenson, A. F. Morpurgo, and V. Podzorov, Phys. Stat. Sol. (a) 201, 1302 (2004).

18. M. Shiraishi, K. Shibata, R. Maruyama, and M. Ata, Phys. Rev B, **68**, 235414 (2003).

Figure captions

Fig. 1. (a) Schematic representation of $C_{88}(C_2(7))$ and cross sectional view of C_{88} FET device. (b) Time-of-flight (TOF) mass spectrum of the purified sample. (c) I_D-V_{DS} and (d) I_D-V_G plots at V_{DS} = 20 V for C_{88} FET at 300 K. Closed circles refer to the points measured at V_G = -30 ~ 100 V.

Fig. 2. V_G dependence of μ for the C_{88} FET at 300 K.

Fig. 3. (a) I_D-V_{DS} and (b) I_D - V_G plots at V_{DS} = 20 V for C_{88} FET at 230 K. Closed circles refer to the points measured at V_G = -30 ~ 100 V. Plots of (c) μ - T and (d) V_T - T. ln μ - 1/T plot in the inset of (c).

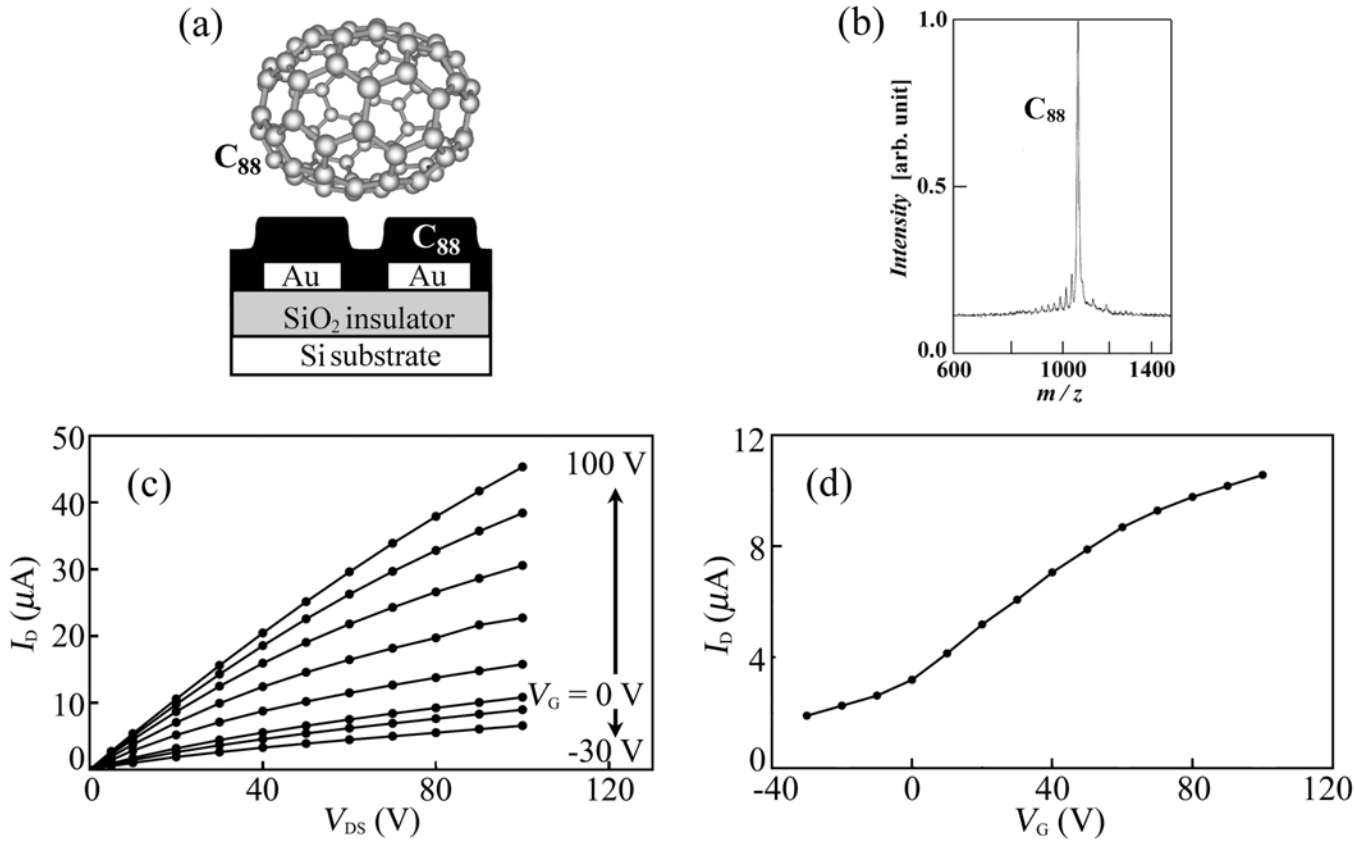
(a)
C88
C88
Au
Au
SiO2 insulator
Si substrate
(b)
1.0
0.5
0.0
Intensity [arb. unit]
C88
600
1000
1400
m / z
(c)
100 V
VG = 0 V
-30 V
ID (μA)
VDS (V)
0
10
20
30
40
50
0
40
80
120
(d)
ID (μA)
VG (V)
0
4
8
12
-40
0
40
80
120

Figure 1.

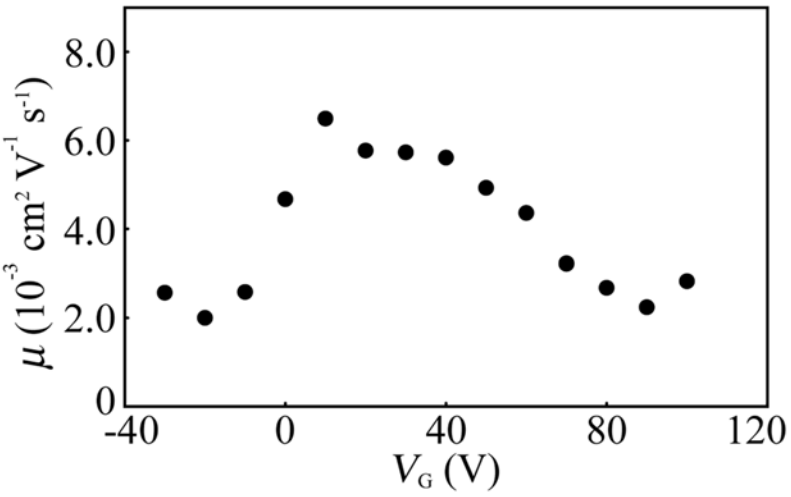

Figure. 2

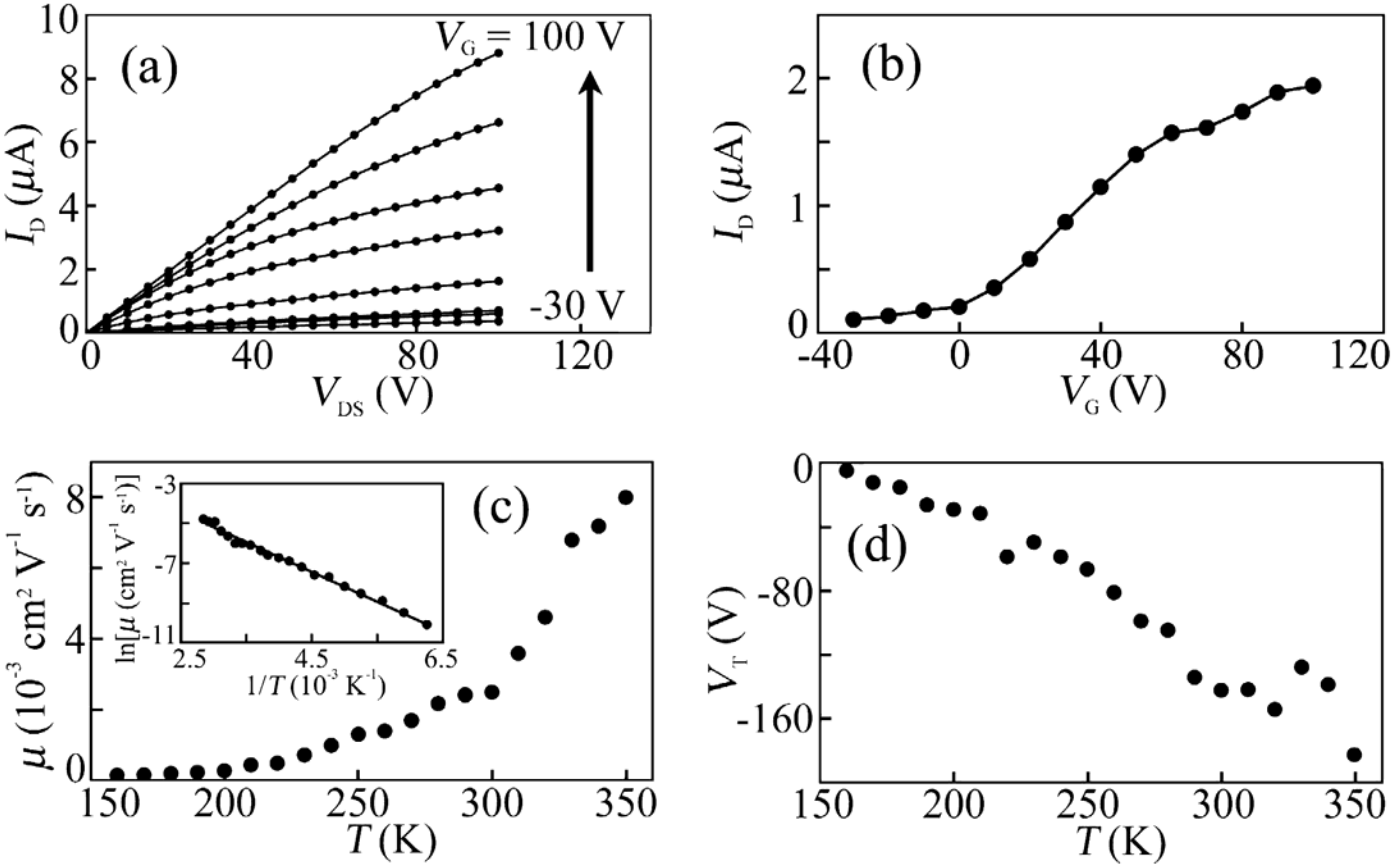
(a)
V_G = 100 V
-30 V
I_D (μA)
V_{DS} (V)
(b)
I_D (μA)
V_G (V)
(c)
μ (10^{-3} cm² V^{-1} s^{-1})
ln[μ (cm² V^{-1} s^{-1})]
1/T (10^{-3} K^{-1})
T (K)
(d)
V_T (V)
T (K)

Figure. 3